Supporting Information

Surface-supported 2D heterotriangulene polymers

Marco Bieri,[a] Stephan Blankenburg,[a] Milan Kivala,[b] Carlo A. Pignedoli,[a] Pascal Ruffieux,[a] Klaus Müllen,[b] and Roman Fasel[*ac]

[a] Empa, Swiss Federal Laboratories for Materials Science and Technology, nanotech@surfaces Laboratory,
Ueberlandstrasse 129, CH-8600 Duebendorf, Switzerland

[b] Max Planck Institute for Polymer Research, Ackermannweg 10, D-55128 Mainz, Germany

[c] Department of Chemistry and Biochemistry, University of Bern, Freiestrasse 3, CH-3012 Bern, Switzerland

[*]Corresponding author: roman.fasel@empa.ch

Experimental

Sample preparation and Scanning tunneling microscopy experiments

Sample preparation is performed in a UHV system with a base pressure below 2 x 10^{-10} mbar. Prior to each experiment, the Ag(111) crystal is cleaned by Ar^+ sputtering at 1 kV and annealing at 725 K for 15 min. After sample cleaning, tribromo-substituted dimethylmethylene-bridged triphenylamine (DTPA, detailed information on the synthesis can be found elsewhere[1]) is deposited from resistively heated quartz crucibles held at 425 K, resulting in deposition rates of about 0.1 ML min^{-1} as monitored by a quartz crystal microbalance. For the fabrication of metal-coordination networks, the Ag(111) crystal is held at 200 °C during molecule deposition. Covalent networks are fabricated with the sample held at 300 °C, and ultraflat, i.e. methyl-cleaved, covalent networks form when the precursor is deposited to Ag(111) held at 400 °C. Subsequent to evaporation, a 5-min post-annealing step is applied at the equal sample temperature. The sample is then transferred to the analysis chamber equipped with an Omicron variable-temperature scanning tunnelling microscope (VT-STM) that is cooled with liquid helium, resulting in sample temperatures of about 50 K. STM topographs are acquired in constant-current mode with the stated voltage referring to the electric potential of the sample with respect to the STM tip.

Density functional theory calculations

To gain detailed insight into the conformation of DTPA adsorbed on Ag(111), as well as the structures of the surface-supported metal-coordination and covalent networks, we perform ab initio simulations based on density functional theory (DFT). We use the CP2K code (http://cp2k.berlios.de/) within the mixed Gaussians and plane waves scheme (GPW)[2] and adopt the exchange-correlation Perdew-Burke-Ernzer (PBE) functional.[3] To account for van der Waals interactions we include empirical corrections according to the scheme proposed by Grimme.[4] The atomic potentials are represented via norm-conserving pseudo-potentials of the Goedecker-Teter-Hutter type[5] and the electronic states are expanded in localized Gaussian basis sets (DZVP for surface metal and bromine atoms, and TZV2P for hydrogen and carbon atoms). The cutoff for the plane wave expansion of the total electronic charge density is 280 Ry.

The adsorbate/metal systems are modeled within the repeated slab scheme: A supercell with full periodic boundary conditions contains three atomic layers of Ag(111), the adsorbed molecules and 30 Å of vacuum space. Periodicity in the direction parallel to the substarte surface mimic an infinite surface. The 2D size of the supercell for the different models is dictated by the size of the superstructure varying from 17.86 x 30.94 $Å^2$ in the case of single molecules adsorbed on the Ag(111) slab up to 20.84 x 36.08 $Å^2$ for the metal coordination networks. For each model, we optimize the atomic positions of the molecules and of the first atomic layer of the substrate. Convergence is checked with respect to the thickness of the Ag(111) layer, and we find that the geometric features as well as simulated STM images have adequately converged already with three Ag(111) atomic layers.

To simulate the STM images we use the Tersoff Hamann approximation[6] to a density of charge obtained by summing up contributions from all the Kohn-Sham orbitals within the Fermi level of the system and the experimental bias voltage. A rolling ball algorithm was adopted to mimic the finite experimental resolution.

The transition from metal-coordination to covalent DTPA networks

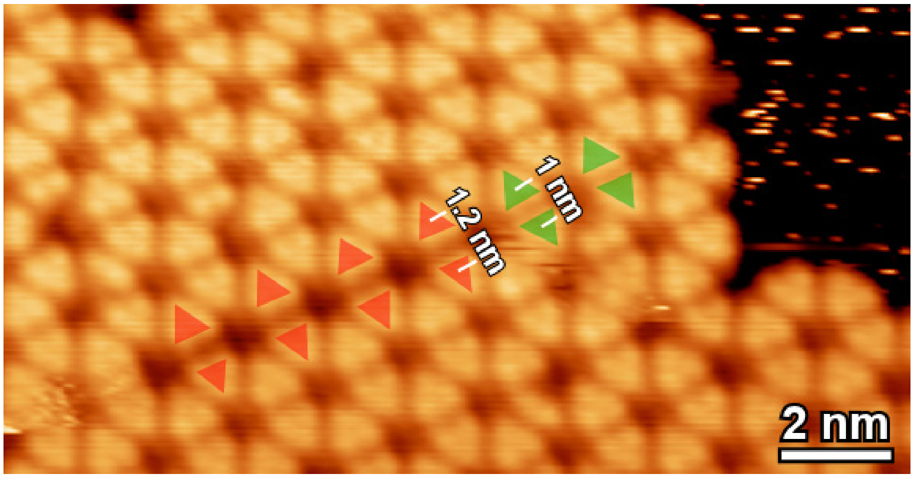

Fig. S1 STM topograph (-2V, 120pA) indicating the transition from coordination toward covalent polymer. Green triangles highlight covalently bonded and red triangles Ag-coordinated molecules in the polymer.

Figure S1 shows an STM topograph acquired after DTPA deposition to Ag(111) held at 275 °C, followed by a post-annealing step at 275 °C for 5 min. The most prominent structural difference between the two types of polymers is the different pore spacing of about 2.1 nm for the coordination polymer compared to 1.7 nm for the covalent network (see Fig. 2 of the manuscript). A prominent boundary, where the difference between Ag-coordinated and covalently bonded species can most easily be recognized, is identifiable in the topograph shown in Fig. S1. Green triangles, with a derived center-to-center distance of about 1 nm, indicate covalently bonded molecules while red triangles, separated by about 1.2 nm, denote metal-coordinated species. The two intermolecular distances are in excellent agreement with an Ag-coordinated and covalently linked dimer as was verified by DFT simulations (see Fig. 2).

Line profile analysis of coordination and covalent DTPA networks

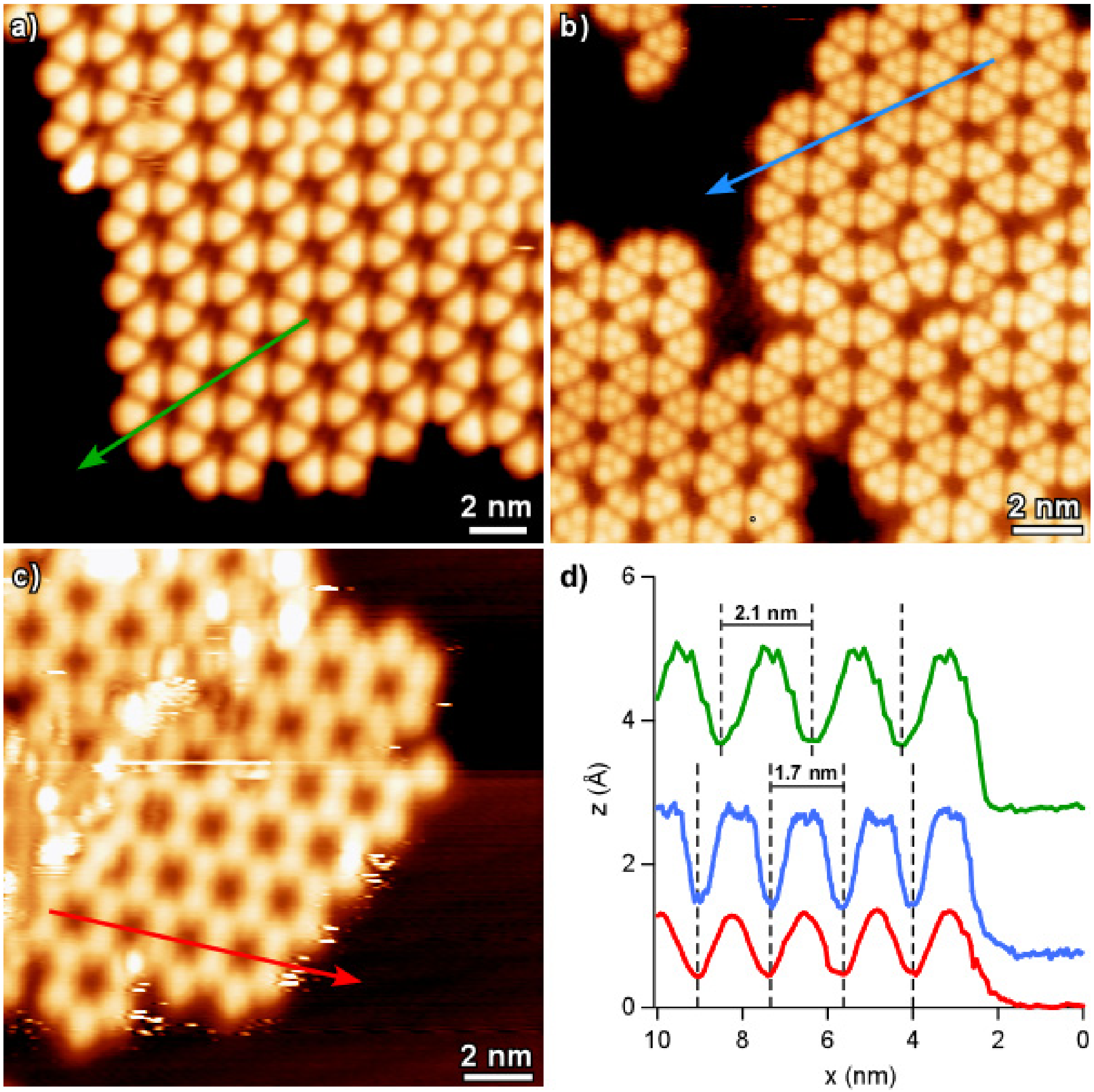

Fig. S2 Line profile analysis of DTPA polymers supported on Ag(111). Line profiles given in (d) are derived along the shown arrows for (a) the coordination network, (b) the covalent network, and (c) the ultraflat, methyl-cleaved covalent network.

To reveal the different pore spacing of the DTPA polymer networks we derive line profiles along the arrows shown in Figs. S2 (a−c). The result is shown in Fig. S2d, where the top trace refers to the coordination polymer, the intermediate trace to the covalent network, and the bottom trace to the ultraflat covalent network with cleaved methyl groups. Comparison of the line profiles reveals equal pore-to-pore periodicity in case of the covalent networks (about 1.7 nm) and the comparably wider porous structure (about 2.1 nm periodicity) of the coordination polymer.

Additional DFT calculations for DTPA and the 2D polymer networks supported on Ag(111)

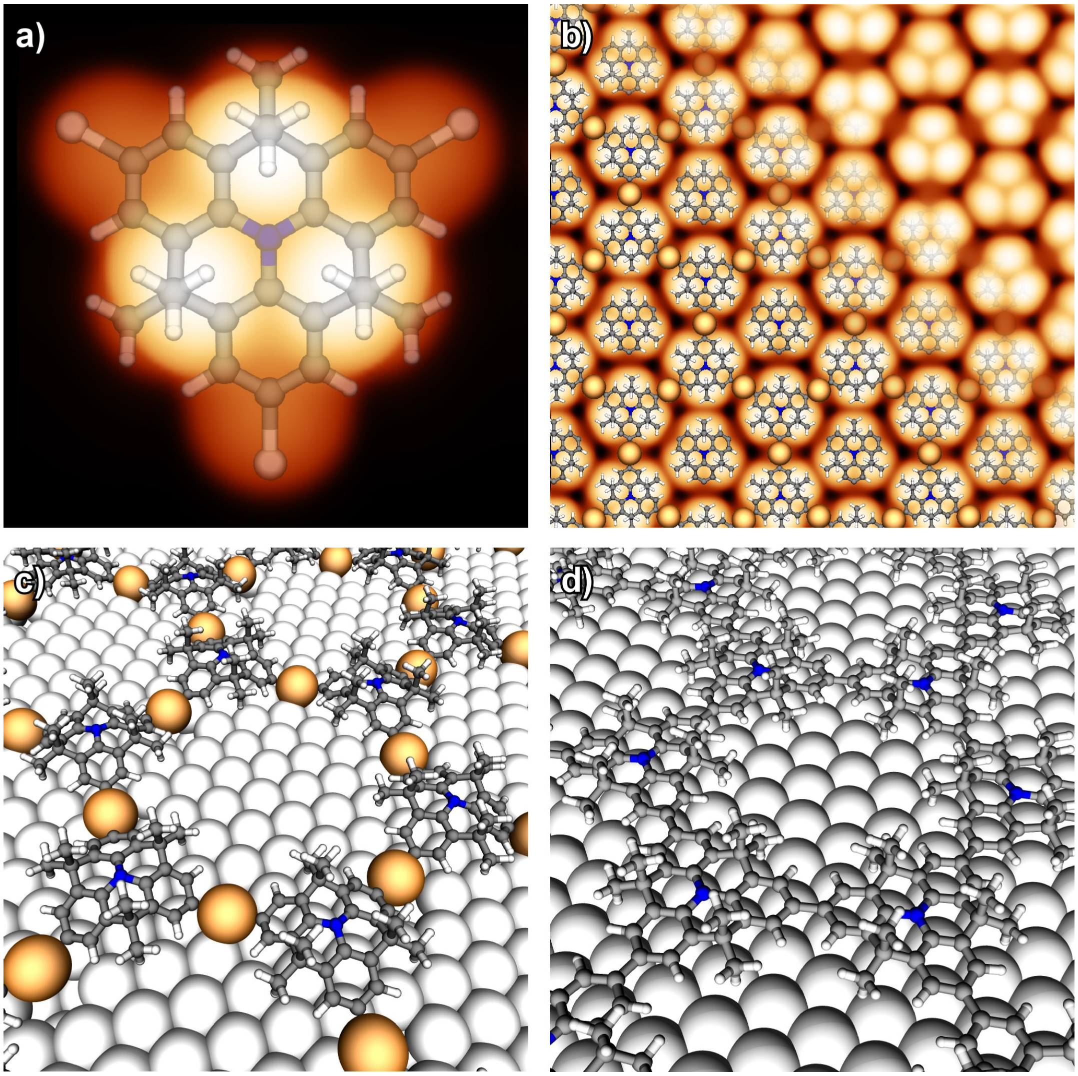

Fig. S3 (a) DFT calculation with superimposed STM simulation of tribromo-substituted DTPA supported on Ag(111). (b) DFT calculation with overlaid STM simulation of the coordination network, with additional DTPA molecules trapped in the pores. (c), (d) Perspective views of coordination polymer (c) and of covalent network (d) as determined from DFT calculations. The elevated Ag atoms of the coordination polymer (c) are highlighted in yellow.

In Fig. S3 we present supplementary DFT results for the precursor and the polymer networks. Tribromo-substituted DTPA adsorbed on Ag(111) is shown in Fig. S3a, where the model is overlaid by the STM simulation obtained within the Tersoff Hamann approximation. As is the case of the surface-stabilized radical (Fig. 1d), the three upstanding methyl units contribute most significantly, and Br atoms with much less intensity to the STM simulation. As a consequence, a clear discrimination between the radical and the brominated species is difficult to make in the experimental data (Fig. 1c). However, as discussed in the text, the arrangement of the molecules on the surface indicates that some of the latter are (at least partially) dehalogenated, as is the case for the highlighted dimer in Fig. 1c, which is separated by only 1.2 nm. In contrast, a significantly increased intermolecular distance of 1.54 nm is found by DFT for bromo-substituted dimers.

Figure S3b shows a model and corresponding STM simulation of the coordination network with "filled" pores, which are experimentally observed in particular in the vicinity of step edges (Fig. 2a). To gain a deeper insight into this structure, we use a commensurate Ag(111) 7x7 unit cell containing three DTPA radicals (two were used for the regular "empty" network) to model the extended coordination polymer with filled pores. After structure optimization, we find that the network takes equal lattice constants than the regular polymer, and that an additional DTPA radical perfectly "fits" into an empty pore. This is possible only in case of the coordination polymer - the pores of the covalent network are too small to accommodate a further molecule, which is in agreement with experimental observation.

To further clarify the structural models shown in Figs. 2d and 2e, we present in Figs. S3c and S3d perspective views of the metal-coordination and covalent networks, respectively, as determined from DFT calculations.

Finally, we like to comment on the structural model of the ultraflat DTPA polymer shown in Fig. 2f. For the DFT calculations, we substitute all CH_3 groups with hydrogen and find that a stable, surface-supported network evolves after structure optimization, of which the STM simulation (Fig. 2f) is in excellent agreement with experiment (Fig. 2c). However, it is important to mention that the exact chemical state of this ultraflat polymer cannot be resolved in detail. For example, a stabilization of the cleaved CH_3 groups by the surface rather than hydrogen substitution may represent another possible scenario.

References

1. Z. Fang, T. L. Teo, L. P. Cai, Y. H. Lai, A. Samoc and M. Samoc, *Organic Letters*, 2009, **11**, 1-4.
2. J. VandeVondele, M. Krack, F. Mohamed, M. Parrinello, T. Chassaing and J. Hutter, *Computer Physics Communications*, 2005, **167**, 103-128.
3. J. P. Perdew, K. Burke and M. Ernzerhof, *Phys. Rev. Lett.*, 1996, **77**, 3865-3868.
4. S. Grimme, J. Antony, S. Ehrlich and H. Krieg, *Journal of Chemical Physics*, 2010, **132**, 154104.
5. S. Goedecker, M. Teter and J. Hutter, *Phys. Rev. B*, 1996, **54**, 1703-1710.
6. J. Tersoff and D. R. Hamann, *Phys. Rev. Lett.*, 1983, **50**, 1998-2001.